AIAA JOURNAL
Vol. 44, No. 11, November 2006

Relaminarization on Swept Leading Edges Under High-Lift Conditions

P. R. Viswanath* and R. Mukund†
National Aerospace Laboratories, Bangalore 560 017, India
R. Narasimha‡
Jawaharlal Nehru Centre for Advanced Scientific Research, Bangalore 560 064, India
and
J. D. Crouch§
Boeing Commercial Airplanes, Seattle, Washington 98124

DOI: 10.2514/1.20035

Detailed experiments were made to gain an improved understanding of relaminarization on swept wings under high-lift conditions. Two swept wings with different airfoil sections and flaps were tested, and measurements were made consisting of surface-pressure distributions and wall shear-stress fluctuations in the leading-edge zone. Measurements were made at a chord Reynolds number of 1.3×10^6 with wing-sweep angles of 45 and 60 deg and model incidence varied in the range of 3 to 18 deg in discrete steps. Following the attachment-line transition, the turbulent boundary layer relaminarized under certain conditions due to the acceleration around the wing's leading edge. Broad features of relaminarization and subsequent retransition are discussed based on wall shear-stress-fluctuation data. The present dataset shows that relaminarization is likely if the maximum value of the acceleration parameter K_s (evaluated along the external inviscid streamline) is greater than about 3×10^{-6}, in agreement with earlier findings. Much higher maximum values of K_s result in significant reduction of intermittency during relaminarization. After relaminarization, the boundary layer retransitions across a separation bubble. Characteristics of the postrelaminarization separation bubbles are shown to be similar to those of bubbles occurring in more pristine laminar boundary layers.

Nomenclature

C_p	=	surface-pressure coefficient based on freestream conditions
c	=	airfoil chord along tunnel freestream direction
$\bar{e}$	=	rms value of wall shear-stress fluctuation, V
e'	=	wall shear-stress fluctuation, V
K	=	$(\nu/U^2)(\delta U/\delta x)$, 2-D definition
$\bar{K}$	=	$(\nu/W_e^2)(\mathrm{d}U_e/\mathrm{d}s)$
$\bar{K}_{\text{ave}}$	=	$1/s \int_0^s \bar{K}(s)\,\mathrm{d}s$
K_l	=	local lateral acceleration parameter, $(\nu/Q_e^2)(\mathrm{d}U_e/\mathrm{d}s)\sin^2\psi_e$
K_s	=	local streamwise acceleration parameter, $(\nu/Q_e^2)(\mathrm{d}U_e/\mathrm{d}s)\cos^2\psi_e$
Q_e	=	local freestream velocity
Q_∞	=	freestream velocity far upstream
Re_c	=	freestream Reynolds number based on c
s	=	distance measured along airfoil surface normal to the leading edge, with the origin at the leading edge
U	=	local freestream velocity, 2-D flow
U_e	=	component of Q_e normal to the wing's leading edge
W_e	=	spanwise component of Q_e
W_∞	=	spanwise component of Q_∞
x	=	airfoil streamwise coordinate with the origin at the leading edge
x_s	=	coordinate tangential to the external inviscid streamline
z_s	=	coordinate normal to x_s
α	=	wing incidence
γ	=	intermittency function
Λ	=	wing sweep
ν	=	kinematic viscosity

Presented as Paper 99 at the 42nd AIAA Aerospace Sciences Meeting & Exhibit, Reno, Nevada, 5–8 January 2004; received 16 September 2005; revision received 5 May 2006; accepted for publication 10 May 2006.

*Head, Experimental Aerodynamics Division. Associate Fellow AIAA.
†Scientist, Experimental Aerodynamics Division.
‡Chairman, Engineering Mechanics Unit. Fellow AIAA.
§Boeing Technical Fellow. Member AIAA.

I. Introduction

THE flow past a swept wing with its high-lift flap system deployed can be quite complex involving three-dimensionality boundary-layer transition by different mechanisms (e.g., attachment-line contamination, crossflow, and Tollmien–Schlichting instabilities), relaminarization, and confluent wakes. It has been suggested [1–3] that attachment-line contamination (ALC) and relaminarization (RL) near the leading edge of swept wings can cause complicated scale effects under high-lift conditions. Improved understanding of this phenomenon is needed to be able to accurately predict the wing's aerodynamic performance (e.g., maximum lift coefficient, $C_{L\,\max}$) from the wind tunnel to flight Reynolds numbers.

ALC is typically caused by contamination due to large-scale turbulence emanating from the fuselage boundary layer, and early studies on the subject included a criterion for ALC reported by Pfenninger [4] and Cumpsty and Head [5]. The relevant Reynolds number [4–6] characterizing ALC is $\bar{R} = W_\infty \eta/\nu$, where $\eta = (\nu/U')^{0.5}$ represents a characteristic boundary-layer thickness along the attachment line (ATL) and U' is the inviscid velocity gradient normal to the ATL at the edge of the boundary layer. Available results suggest [4–7] that, if $\bar{R} > 250$, the turbulence will be self-sustaining, causing the ATL as well as the flow downstream of it to become turbulent.

There is now sufficient evidence [1–3,7–14] to show that, following ALC on a swept-wing leading edge, the turbulent boundary layer can relaminarize due to the strong acceleration around the leading edge. The acceleration parameter K, widely used to characterize 2-D relaminarizing boundary layers at low speeds, was first proposed for the occurrence of relaminarization on swept

wings by Beasly [8], except that the parameter was evaluated along the external inviscid streamline; recent studies [9–14] examining relaminarization on swept wings at high-lift have continued to rely on the usefulness of this parameter K. The possible additional effect of leading-edge convex surface curvature in promoting relaminarization has not been examined in any detail. However, recent experimental studies [15–17] have indicated strong effects of convex surface curvature combined with streamwise acceleration in promoting relaminarization in 2-D boundary-layer flows.

Arnal and Juillen [7] presented some experimental evidence from a wind-tunnel study examining ALC and subsequent RL on a swept RA16SC1 airfoil model at low speeds; their study included measurement of chordwise surface-pressure distributions at several spanwise locations and data from surface mounted hot-films in the wing's leading-edge zone (limited to within 2% chord on either side of the attachment line). Under certain freestream velocity conditions, their results showed that turbulent spots at the attachment line decayed around the leading edge due to relaminarization. These observations were found consistent with relatively large values of the acceleration parameter K (about 9×10^{-6}) in the leading-edge region. Van Dam et al [3] studied aspects of ALC and subsequent relaminarization on the Boeing 737-100 aircraft high-lift system under flight conditions using measured surface-pressure distributions on the wing. The Reynolds number (based on the wing's mean aerodynamic chord) varied in the range of $10.2–20.2 \times 10^6$. Their analysis suggested significant regions of relaminarized flow on all flap elements, but no measurements of the state of the boundary layers were made. In subsequent flight measurements employing hot-films, Van Dam et al [10,11] observed relaminarization around the slat and main-wing leading edges under certain flight conditions; the Reynolds numbers were in the range of $10.5–21.8 \times 10^6$ in these tests. The maximum value of K was in excess of 3×10^{-6} for these cases, and Van Dam et al [10,11] suggested that K was a useful parameter for correlating the occurrence of relaminarization in swept-wing flows as well. Under the European high-lift (EUROLIFT) research project in high-lift aerodynamics, specific experimental and numerical studies were carried out on a generic high-lift swept-wing configuration [12–14]. The major objective was to provide a database for transition-prediction tool developers for the assessment of numerical methods. The experiments were made in the ONERA F1 pressurized wind tunnel on a three-element airfoil model instrumented with several spanwise rows of static pressure taps and hot-films, suitably distributed on the slat, main airfoil, and flap. The measurements revealed partial relaminarization on the slat's upper side only for chord Reynolds numbers greater than 6×10^6 and high angles of attack; the (max) value of the acceleration parameter (K) was around 5×10^{-6}. The data available on swept-wing relaminarization are thus very limited, although there is considerable interest in the problem from both scientific and technological points of view. Some of the important issues include the conditions that lead to the relaminarization around the leading edge; the most suitable criterion to characterize relaminarization in three-dimensional flows; the relative importance of the rate and extent of the acceleration; and possible convex surface curvature effects on relaminarization.

The major objective of the present work is to generate a useful set of experimental data on swept-wing relaminarization to enable improved understanding leading to better flow modeling for calculation methods. Detailed experiments have been performed on two swept wings at low speeds. The strategy employed involves generation of an attachment-line transition at wind-tunnel Reynolds numbers (similar to the study of Arnal and Juillen) and documentation of the broad features of relaminarization and subsequent retransition to turbulent flow using a large number of surface mounted hot-films in the leading-edge zone. The wing incidence was varied to generate different levels of acceleration in the nose region. Surface-pressure distributions on the wing have been measured, and a surface oil-flow technique was used to infer important features like the state of the attachment-line boundary layer or the occurrence of laminar-separation bubbles causing a retransition to turbulent flow. Different criteria for the occurrence of relaminarization based on inviscid flow parameters have also been examined.

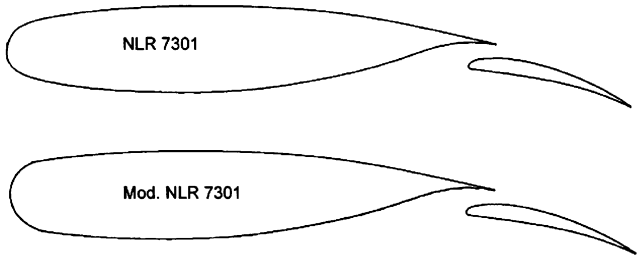

Fig. 1 Sketch showing swept-wing geometric details.

II. Experiments

A. Test Facility

Experiments were carried out in the National Aerospace Laboratories' 1.5×1.5 m low-speed wind tunnel in which the freestream speed can be varied in the range of 10–50 m/s. The speed control is better than 1%, and the freestream turbulence is less than 0.12% in the above speed range.

B. Model Configurations

Two swept-wing configurations were chosen for this study, as shown in Fig. 1. The geometric details for the wing configurations are shown in Table 1. All the tests were carried out at a (nominal) freestream velocity of 48 m/s, at which the chord Reynolds number was about 1.3×10^6. The model incidence was varied in the range of 0–18 deg in discrete steps. The Nationaal Lucht-en Ruimtevaart Laboratorium (NLR), The Netherlands, 7301 airfoil-flap geometry, swept at 45 deg (wing A), was chosen for the first set of measurements because the aerodynamic characteristics of the airfoil with flap (in two-dimensional flow) were available in the literature [18]. For the second set of measurements, the NLR 7301 airfoil geometry was modified near the leading edge with a larger nose radius, and the wing was swept at 60 deg (wing B) to promote a turbulent attachment line even at moderate angles of attack. All the wing models had a span of 2.5 times the airfoil chord to approximate infinite sweep and an end plate to avoid tip effects. The inboard section of the wing was mounted on a base plate with a 2-D wedge in front (Fig. 2) to take advantage of the tunnel turbulent boundary layer for promoting attachment-line contamination.

C. Model Instrumentation

The wing models were constructed out of glass fiber composites and instrumented with two streamwise rows (AA and BB) of static pressure ports (about 50 in each row) on either side of the model midspan (Fig. 2). The model's surface-pressure distributions were measured using low-pressure Setra transducers (with a range of 200–540 mm of water) integrated with 48-port Scanivalves.

Single element surface hot-films (manufactured by Micro Measurements Co.), having a resistance of 50 Ω, were employed as primary diagnostics for inferring attachment-line contamination, subsequent relaminarization, and retransition. Typically 10–12 gauges were bonded to the surface in the leading-edge zone (within the first 15% chord on the pressure and suction surfaces); these gauges were staggered in the spanwise direction (to avoid any disturbance originating from the upstream gauges affecting those downstream) and were located in the midspan region between AA and BB. The gauges were glued so that the active film was nearly normal to the local surface flow direction, which was found to be relatively less sensitive to α over a range of model incidence angles (6–18 deg). The hot-film measurements were made employing DISA, Inc., 55M constant-temperature anemometer systems at a

Table 1 Geometric details for the tested swept-wing configurations

Model	Designation	Airfoil chord, m	Extended chord with flap, m	Sweep
NLR 7301	A	0.450	0.54	45 deg
Modified NLR 7301	B	0.4275	0.512	60 deg

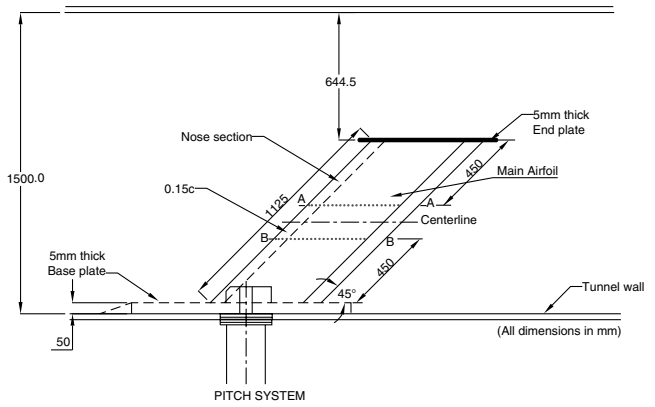

Fig. 2 Schematic of the swept-wing model located in the tunnel: sweep = 45 deg.

fixed overheat ratio of 1.20, and the unsteady signals were amplified by a fixed gain. The unsteady signal from each gauge was acquired at a sampling rate of 2 kHz for about 30 s (earlier work showed that most of the energy in the wall shear-stress signals was in frequencies below 1 kHz). These signals provided information on the nature of the boundary layer through the rms quantities, intermittency values, and spectra. Data acquisition and processing was performed using a Pentium PC.

Surface flow visualization studies in the leading-edge zone were carried out using a mixture of titanium dioxide in oil to detect features like the attachment line and laminar-separation bubbles; information on surface streamlines was used to fix the orientation of hot-film gauges (as mentioned earlier).

D. Accuracy of Measured Data

The model surface-pressure distributions were measured using Setra pressure transducers, which were accurately calibrated. The overall uncertainty in C_p, estimated taking into account component errors and data repeatability, was $\Delta C_p = \pm 0.5\%\ C_p$ (20 to 1).

III. Results and Discussion

Before presenting the experimental results, it is appropriate to define all the different flow parameters relevant to the present study.

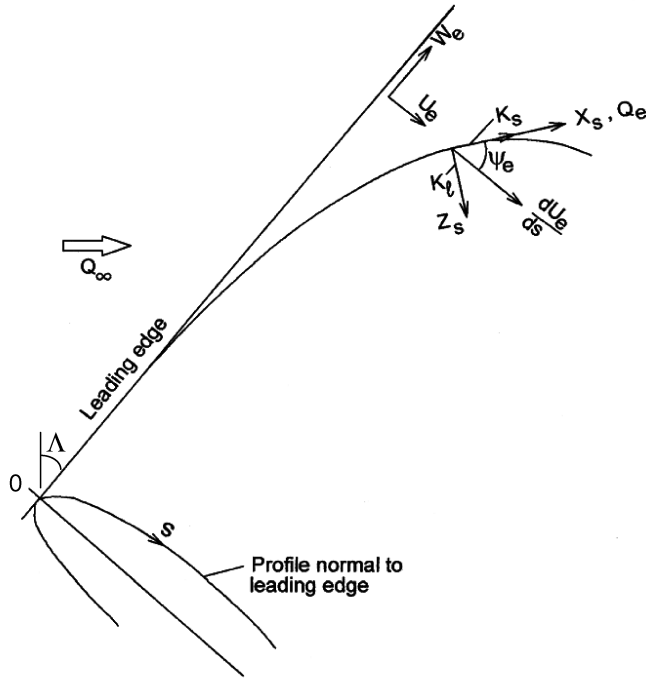

Fig. 3 Sketch defining geometry and axis system.

A schematic of the coordinate system used along with a definition of certain flow parameters is presented in Fig. 3. The different acceleration parameters that we use in this study are also defined in the nomenclature for this paper. We define K_s using flow variations on the airfoil section normal to the wing's leading edge (see Fig. 3 and the nomenclature), and similarly we define the lateral acceleration parameter K_l (normal to K_s). Note that K_s is equivalent to K evaluated along the external inviscid streamline on a swept wing. With a model span of 2.5 times the airfoil chord, very good spanwise uniformity of surface pressures was observed along AA and BB (Fig. 2) except for small departures ($\Delta C_p < \pm 0.20$) around $C_{p\,\min}$ at higher incidence; in what follows the data measured along BB will be presented. For estimating the flow properties on the swept wing from surface-pressure measurements, we have assumed that the spanwise velocity component W_e ($=W_\infty$) is a constant given by $Q_\infty \sin \Lambda$, implying infinite sweep conditions.

A. Attachment-Line Characteristics

Figure 4 shows the variation of the attachment-line Reynolds number, $\bar{R}$, with incidence on wings A and B; $\bar{R}$ was calculated using the detailed methodology adopted by Van Dam et al [3]. $\bar{R}$ generally shows an increase with α, a trend to be expected because the attachment line moves aft from the leading edge to a region of smaller surface curvature on the lower surface. $\bar{R}$ values are higher than 250 virtually all across the incidence range for wing B and for $\alpha > 12°$ on wing A. Test conditions having $\bar{R} > 250$ may be expected to have a turbulent attachment line on the wing because the attachment line originates from the turbulent tunnel-wall boundary layer.

In this paper, we examine the detailed results for three test conditions and draw some major conclusions from these results. The test cases include $\alpha = 15$ and 17 deg on wing A and $\alpha = 12$ deg on wing B, all having turbulent attachment-line conditions.

B. Chordwise Pressure Distributions and Acceleration in the Leading-Edge Zone

Results of chordwise pressure distributions and variation of the acceleration parameter K_s (along the external inviscid streamline), at $\alpha = 15$ and 17 deg on wing A, are displayed in Figs. 5 and 6 respectively. In these figures, $x/c = 0$ is the leading edge, $x/c < 0$ is the lower surface, and $x/c > 0$ is the upper surface. The pressure distributions show features typical of high-lift conditions [3,11]; the suction peak and the maximum value of K_s are relatively higher at $\alpha = 17$ deg because of larger incidence. A laminar-separation bubble (LSB) with a streamwise extent of 2–3% chord was a feature

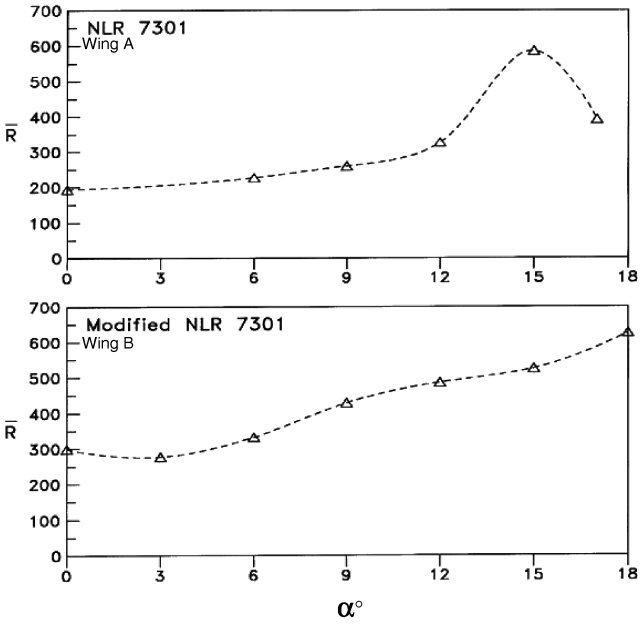

Fig. 4 Variation of attachment-line Reynolds number with incidence.

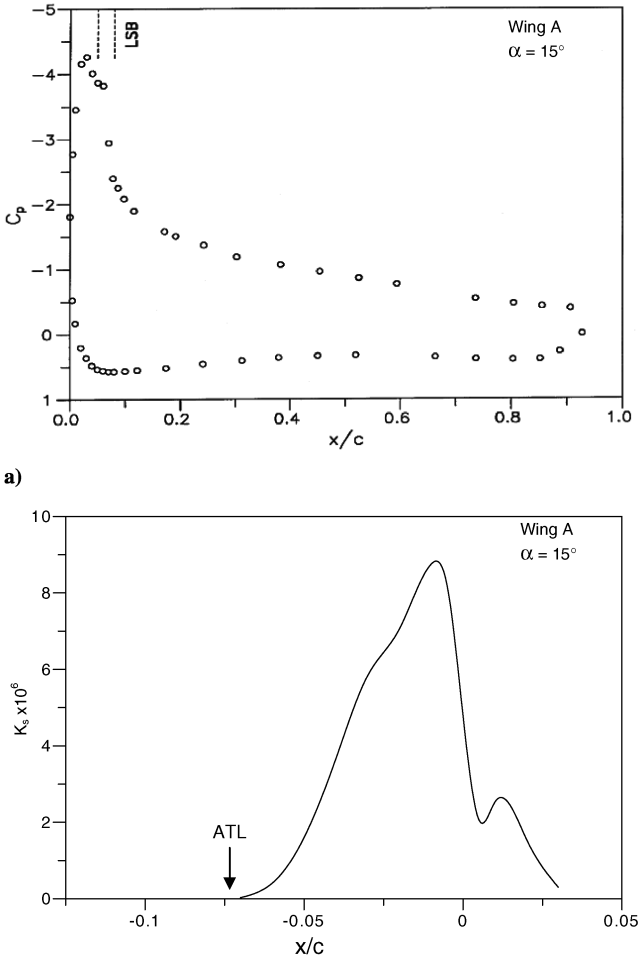

Fig. 5 Chordwise surface-pressure distributions and acceleration parameter K_s: wing A, $\alpha = 15$ deg.

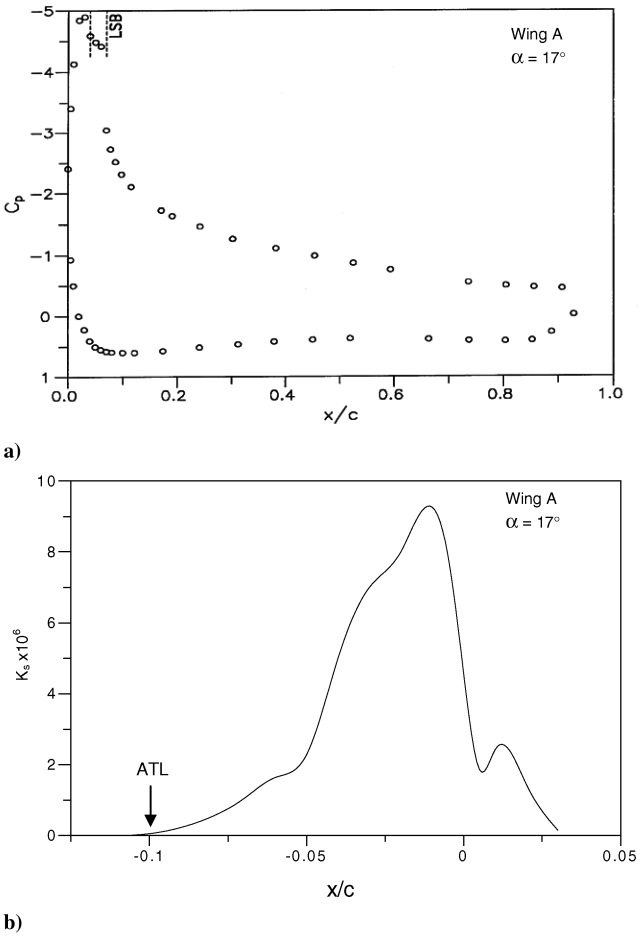

Fig. 6 Chordwise surface-pressure distributions and acceleration parameter K_s: wing A, $\alpha = 17$ deg.

across the α range studied on this wing; the position of LSB, as inferred from surface flow visualization studies, is marked in Figs. 5a and 6a. Samples of LSB features on wing A are shown in Fig. 7; in these photographs, the wing's leading edge is aligned to the vertical, and the arrow indicates the direction of the oncoming flow. S and R represent separation and reattachment of the bubble (Fig. 7). Results at $\alpha = 12$ deg on wing B are shown as a representative case for that wing (Fig. 8). The suction peak and maximum value of K_s reached were much lower on wing B than on wing A because of the larger nose radius (lower nose curvature); even at the highest incidence of $\alpha = 18$ deg, the maximum value of K_s was about 3.9×10^{-6}. As on wing A, surface flow visualization studies also revealed a laminar-separation bubble for $\alpha > 3$ deg on this wing.

C. Features of Hot-Film Signals around the Wing's Leading Edge

The characteristics of hot-film signals obtained in the leading-edge zone at $\alpha = 15$ and 17 deg on wing A are presented in Figs. 9 and 10, respectively; also included in these figures are the corresponding streamwise variations of the intermittency function and the rms value of the signal $\bar{e}$. In these figures, $x/c = 0$ is the leading edge, $x/c < 0$ is the lower surface, and $x/c > 0$ is the upper surface. On each wing, the ac signal amplification for all the gauges was the same so that absolute changes in the amplitude levels, as the flow goes around the leading edge, can be seen.

The wall shear-stress signals [Figs. 9a and 10a] show a turbulent character in the close vicinity of the attachment line (gauge A′ and A in Figs. 9 and 10), as may be expected from the prevailing large values of $\bar{R}$ (Fig. 4). Significant quenching of turbulence is observed in the acceleration zone suggesting relaminarization. Retransition of the relaminarized boundary layer is triggered by the presence of a LSB occurring immediately downstream of the suction peak (Figs. 5 and 6).

The intermittency function was determined using a method developed for calculating intermittency during laminar-turbulent transition from hot-wire signals [19]. We have used the same method here for analyzing the hot-film signal during relaminarization, although the signals are often noisy because of the residual fluctuations in the relaminarized flow. In this method the ac signal is differentiated twice, squared, and γ calculated using a threshold value obtained from its probability density function. The methodology as used here gives a useful indicator of intermittency

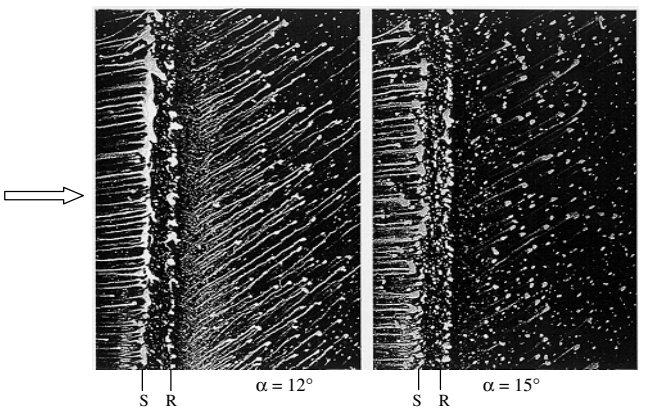

Fig. 7 Surface flow features showing a separation bubble on the wing's upper surface.

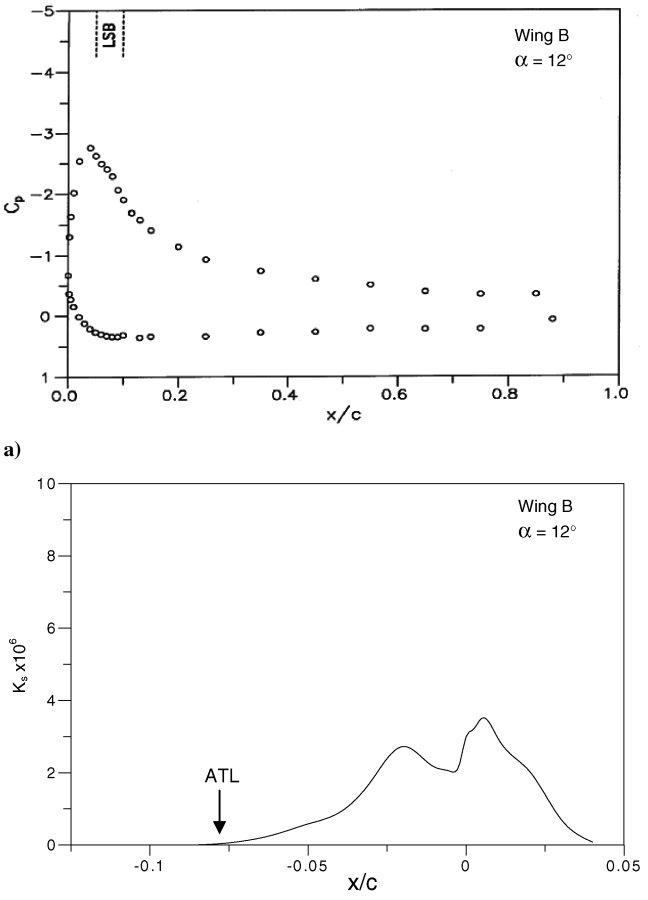

Fig. 8 Chordwise surface-pressure distributions and acceleration parameter K_s: wing B, $\alpha = 12$ deg.

that agrees broadly with a visual inspection of signals. The uncertainty in the estimation of γ is generally expected to be small near the extremes ($\gamma \to 0$ and $\gamma \to 1$). For moderate values of γ, error bars are shown in Figs. 9–11 that reflect the sensitivity to the variation in the chosen threshold values.

The distributions of γ and $\bar{e}$ for the hot-film signals (Figs. 9b, 9c, 10b, and 10c) show that relaminarization is associated with low values of γ (<0.2). These observations suggest that higher acceleration levels in the leading-edge zone result in low values of γ. The $\bar{e}$ values show the expected trends (Figs. 9c and 10c), namely, an appreciable reduction during relaminarization and a significant increase during retransition, followed by a reduced level associated with a developing turbulent boundary layer.

The dramatic reduction in γ during the initial phase of acceleration (gauge B in Figs. 9 and 10), where K_s is still under 3×10^{-6}, suggests that relaminarization may be aided by viscous dissipation [20] and lateral acceleration. The hot-film signals (e.g., gauge D in Fig. 9 and gauges D and E in Fig. 10) show a small growth in amplitude towards retransition but again are suppressed by the strong acceleration with K_s reaching values as high as 9×10^{-6}. It is possible that relaminarization is occurring in two stages, initially assisted by viscous dissipation and lateral acceleration and later by the action of strong streamwise acceleration. More discussion on this will be reported elsewhere.

Hot-film traces, γ and $\bar{e}$ distributions at $\alpha = 12$ deg on wing B, are shown in Fig. 11. These results are typical of what was observed on this wing at higher α values (15 and 18 deg). The attachment line is turbulent and a fair degree of quenching of turbulence in the acceleration zone around the leading edge is observed. This is followed by retransition across a LSB. In comparison with results on wing A (Figs. 9 and 10), the degree of quenching of turbulence may be seen to be lower, consistent with a relatively smaller maximum

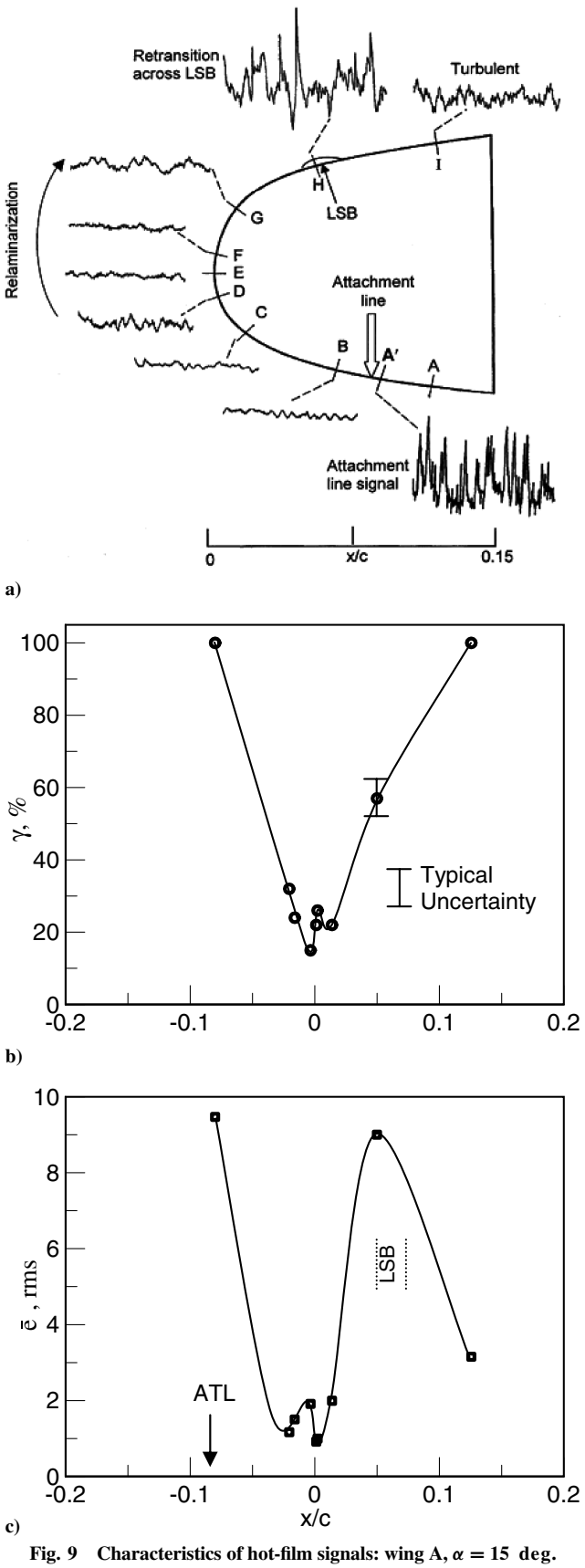

Fig. 9 Characteristics of hot-film signals: wing A, $\alpha = 15$ deg.

value of K_s and its streamwise gradient on wing B (Fig. 8). The presence of a laminar-separation bubble and strong evidence of retransition across the bubble indicates relaminarization of the mean flow. It is well known from studies [20] in 2-D relaminarizing boundary-layer flows that fluctuations do remain during

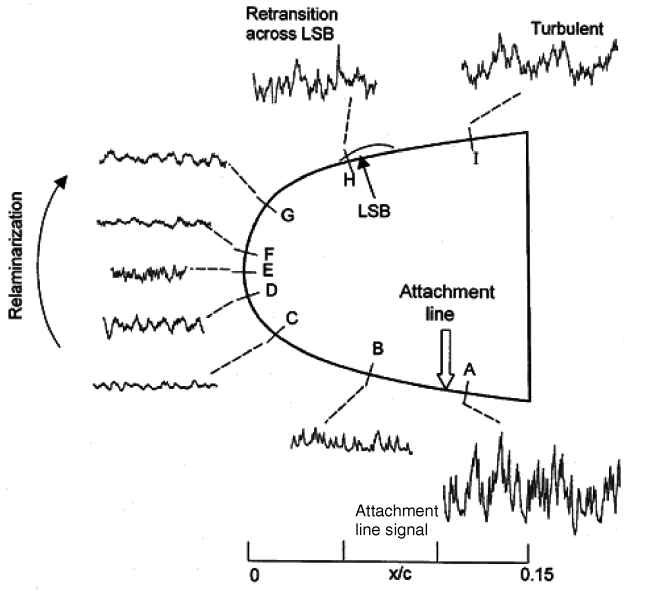

a)

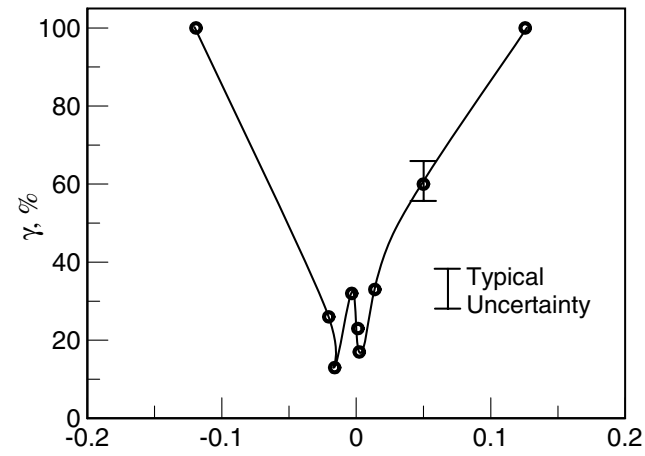

b)

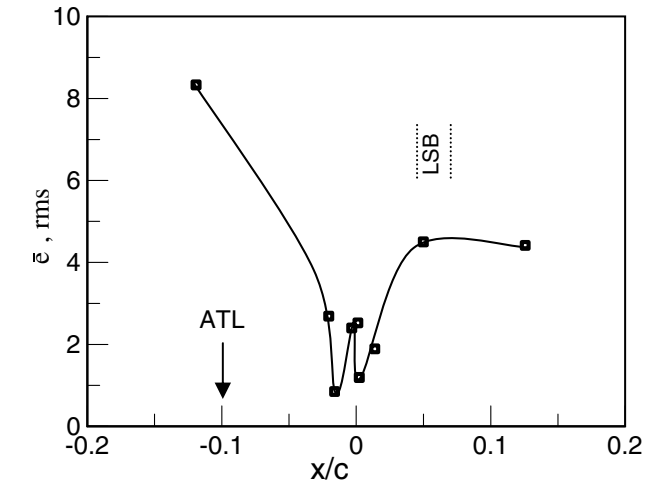

c)

Fig. 10 Characteristics of hot-film signals: wing A, $\alpha = 17$ deg.

relaminarization, but they contribute very little to the dynamics of the mean flow. As may be expected, intermittency values during relaminarization (Fig. 11b) are relatively higher (about 0.70) in contrast with results on wing A. The streamwise variation of $\bar{e}$ (Fig. 11c), however, is qualitatively similar to that on wing A.

D. Spectra of Hot-Film Fluctuations

Power spectra of wall shear-stress signals, as the boundary layer develops around the wing's leading edge, can provide some information on how the fluctuation energy is distributed in frequency among the different flow zones. Spectra at four typical locations representing turbulent attachment line, relaminarization zone, retransition, and developing turbulent boundary layer are presented in Fig. 12 at $\alpha = 15$ deg on wing A and at $\alpha = 12$ deg on wing B; the gauge positions corresponding to these flow zones are indicated in Figs. 9 and 11, respectively. On wing A, the intermittency at relaminarization was indeed low ($\gamma < 0.2$); the reduction in energy level is spectacular all across the frequency range in the relaminarization zone (gauge E). On wing B, where the intermittency level was relatively high (about 0.70) in the relaminarization zone (gauge I), the reduction in energy is only about a factor of 30 at low frequencies (<100 Hz) but is about 10^2 at higher frequencies. An appreciable increase in energy all across the frequency range due to retransition of the relaminarized boundary layer may be clearly observed for both cases.

The interpretation of spectra in relaminarizing or retransitioning flows is not easy because the signal keeps switching between two more or less noisy levels. Nevertheless a comparison of the two sets of spectra in Fig. 12 suggests the following: In the first place, the spectra at ATL (A′ on wing A and C in wing B) are largely similar. The most interesting difference between the two cases is that, except at the attachment line, energy at the higher frequencies is generally higher in wing B than in wing A. Wing B also shows higher intermittency levels (compare Fig. 11 with Fig. 10). This could be explained by the flow switching between two states, both with high fluctuation amplitudes. This would account for the greater spectral density at high frequencies. In contrast, in wing A, intermittency levels can be quite low, and the fluctuations at the low intermittency levels are so small (gauge E) that the drop at high frequencies is dominated by the turbulent part of the signal. The data does not justify a more detailed explanation, but we can conclude that where relaminarization is more nearly complete the drop in the spectral density can be as high as 2 to 3 orders of magnitude depending on the frequency.

E. Criteria for Relaminarization on Swept Leading Edges

In the context of 2-D relaminarizing boundary layers under the action of streamwise acceleration, a variety of criteria for the occurrence of RL have been suggested [20], with many of them based on inviscid flow parameters (e.g., K). An extensive review of the various criteria and the difficulties associated with their use has been summarized by Narasimha and Sreenivasan [20]. Narasimha and Sreenivasan [21] also formulated a successful methodology for calculating the boundary-layer development during the later stages of relaminarization in which the pressure forces dominate the Reynolds shear stress in the flow.

There is virtually no information available on boundary-layer parameters (including wall shear stress) during RL around a swept leading edge. Such measurements are very difficult because of three-dimensionality and the very small boundary-layer thicknesses. Limited studies exist which use surface mounted hot-films (as in the present work) to infer the nature of the boundary layer from wall shear-stress fluctuations. As stated in the introduction, the acceleration parameter K (widely used in 2-D flows) evaluated along the external inviscid streamline has been shown to be a useful correlating parameter for the occurrence of RL on swept wings; the threshold value of K_s often suggested for RL is about 3×10^{-6} (see [3,11]).

We have examined several acceleration parameters based on inviscid flow properties that include K_s, K_l, $\bar{K}$, and $\bar{K}_{\text{ave}}$ (see Fig. 3 and the nomenclature for definition of the K variants). The subscripts s and l correspond to streamwise and lateral strains, respectively. The over bar signifies scaling similar to $\bar{R}$. All the K parameters have in common the velocity gradient along the airfoil contour normal to the leading edge (Fig. 3). Because all test flows with $\bar{R} > 250$ in the present series of experiments showed strong evidence of

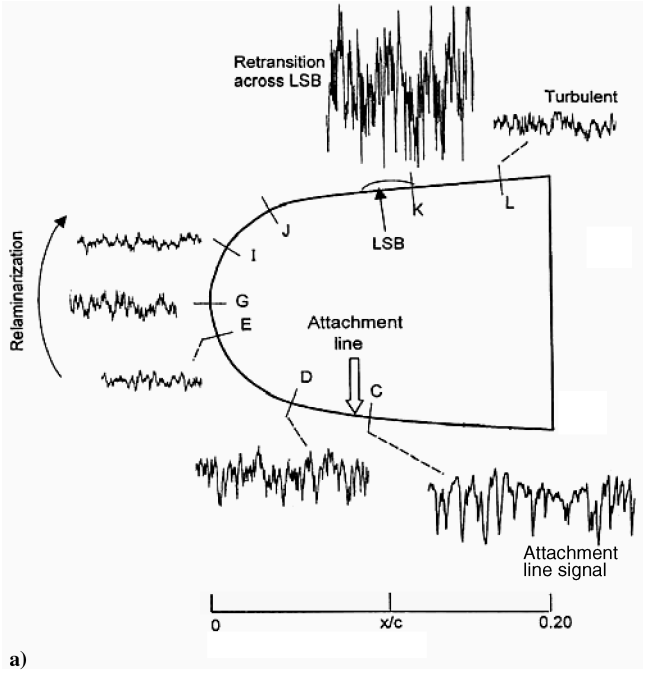

a)

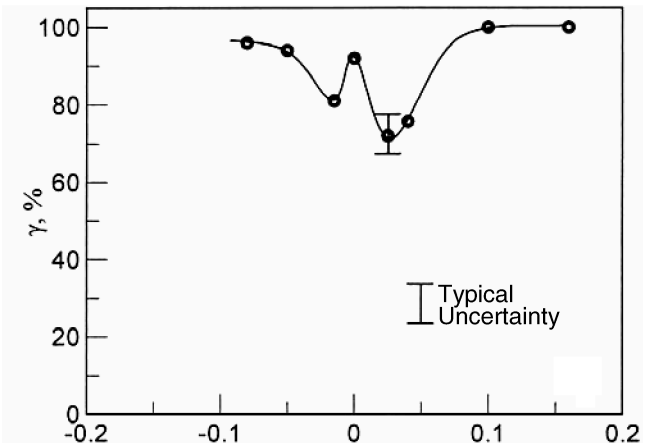

b)

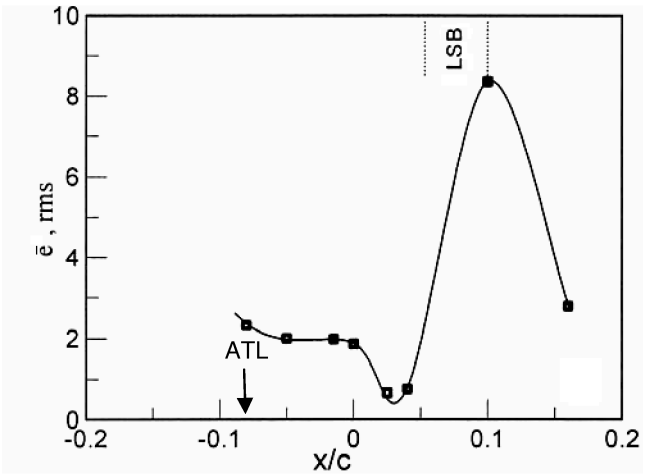

c)

Fig. 11 Characteristics of hot-film signals: wing B, $\alpha = 12$ deg.

relaminarization, the relaminarization boundary could not be established for the different K variants; essentially, the four different K parameters attain different levels at RL.

Having evaluated the different K parameters, we present in Fig. 13 the variations of K_s and $\bar{K}_{\text{ave}}$ for the test flows at $\alpha = 15$ and 17 deg

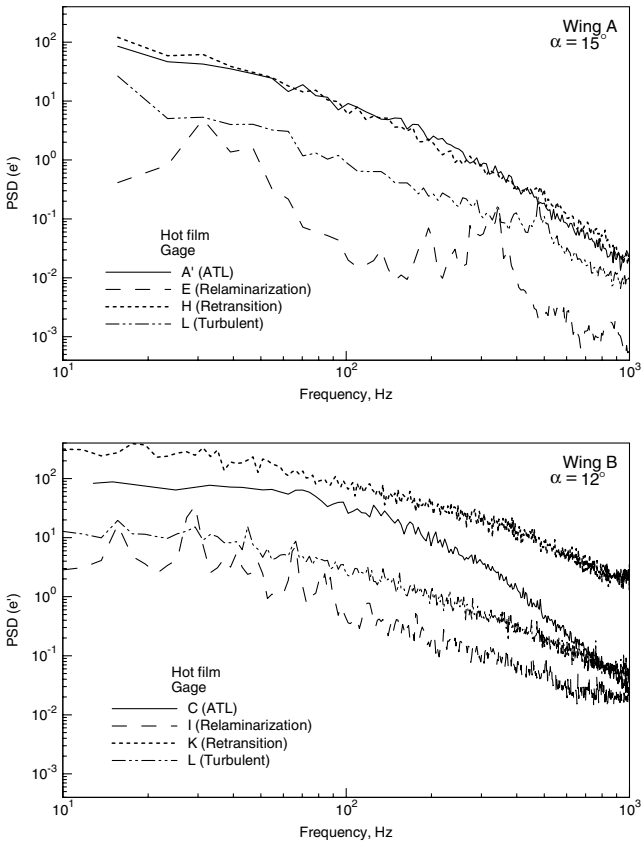

Fig. 12 Power spectra of hot-film fluctuations in different flow zones.

on wing A and $\alpha = 12$ deg on wing B. Also shown in Fig. 13 are the gauge positions where the first minimum in the intermittency value was observed as the boundary layer goes around the leading edge. At $\alpha = 15$ and 17 deg on wing A where RL resulted in low γ (<0.2), the local values of K_s and $\bar{K}_{\text{ave}}$ at gauge C are around 8×10^{-6} and 22×10^{-6}, respectively (Figs. 13a and 13b). The K values at gauge C provide an upper limit for the relaminarization-threshold values because the actual minimum in γ could have occurred upstream, between gauges B and C. An initial value of $\bar{K}_{\text{ave}} = 16 \times 10^{-6}$ on the attachment line is equivalent to $\bar{R} = 250$. Thus, values of $\bar{K}_{\text{ave}} > 16 \times 10^{-6}$ are known to relaminarize the attachment line, which has lateral but not streamwise acceleration. The combination of

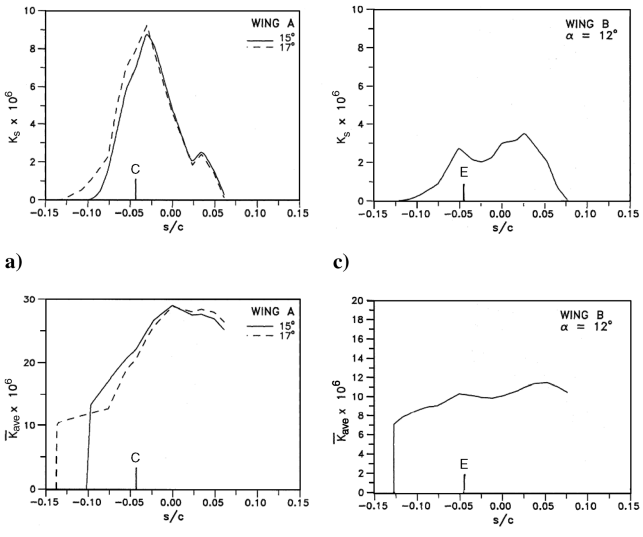

Fig. 13 Streamwise variations of K_s and $\bar{K}$ (average) on wings A and B.

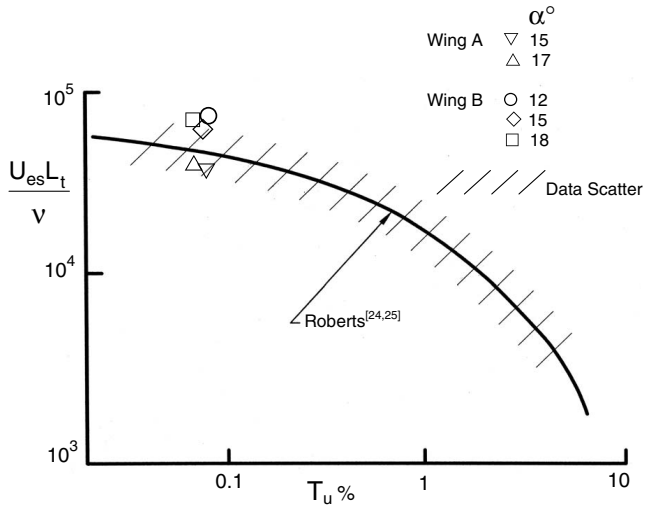

Fig. 14 Comparison of bubble transition Reynolds numbers with correlation from Roberts [24,25].

streamwise and lateral acceleration could be expected to yield a lower threshold value for $\bar{K}_{ave}$.

Flight investigation of relaminarization on the main wing of a Boeing 737-100 aircraft provides further support [11] to the preceding threshold value of K_s associated with low-γ values; values of γ less than 0.1 were observed [11] for the maximum value of K_s above 6×10^{-6}. Based on the limited results available, we may conclude that RL may be accompanied by relatively low γ if the local value of K_s is in excess of about 6×10^{-6}. On wing B, values of K_s and $\bar{K}_{ave}$ at gauge E are much lower (about 3×10^{-6} and 10×10^{-6}, respectively, Fig. 13c and 13d), and RL was associated with a much higher level of intermittency (about 0.7). At other angles of attack on wing B (e.g., 9, 15, and 18 deg), the broad features of RL observed were essentially the same as those reported here at $\alpha = 12$ deg; the maximum value of K_s was about 4×10^{-6} at $\alpha = 15$ and 18 deg, and 3.5×10^{-6} at $\alpha = 12$ deg.

These results suggest that a more fundamental parameter than a member of the K family may be required to identify relaminarization (perhaps the ratio of stress gradients [20,21]). However, this question cannot be resolved here in the absence of more detailed data on boundary-layer thickness and Reynolds stresses in the flows investigated.

F. Separation-Bubble Reynolds Numbers for Retransition

As discussed in Sec. III.B, retransition of the relaminarized boundary layer occurred across a laminar-separation bubble in all cases. A useful correlation for the bubble length is given in terms of the transition Reynolds number, $Re_t = U_{es}L_t/\nu$, where U_{es} is the local velocity at separation (normal to the leading edge) and L_t is the distance from separation to transition. Earlier studies on laminar-separation bubbles have shown that L_t is approximately 0.72 times the bubble length [22]. Here, we assume that this relationship holds for relaminarized boundary layers to estimate the transition Reynolds number from the measured bubble lengths.

Davis et al [23] have shown that the transition Reynolds number of laminar-separation bubbles is well correlated with the freestream turbulent intensity, T_u, scaled by the local boundary-layer edge velocity. Figure 14 shows the transition Reynolds numbers from the current study in conjunction with an empirical relationship of Roberts [24,25], $Re_t = 25,000\log_{10}[\coth(17.32T_u)]$. The hashed area shows the data range from several experiments for laminar bubbles not preceded by relaminarization, as presented by Davis et al [23]. The present data on Re_t, following relaminarization, are in general agreement with the preceding correlation. The data on wing A ($\alpha = 15$ and 17 deg) with low values of γ during relaminarization show excellent agreement, whereas those on wing B ($\alpha = 12$, 15, and 18 deg) have relatively higher values of Re_t (the data at $\alpha = 15$ and 18 deg on wing B have also been included in this plot because they displayed relaminarization features very similar to those at $\alpha = 12$ deg). A useful conclusion that emerges is that the transition Reynolds number correlation can be used with some confidence, even for cases of retransition following relaminarization, if the intermittency levels reached during relaminarization are relatively low ($\gamma \to 0$); this is a strong possibility under certain favorable flight conditions (e.g., $Re_c \sim 10^7$) because the maximum values of K_s attained are quite high (>6–8 $\times 10^{-6}$, see [10,11]).

IV. Conclusions

A detailed experimental program was carried out specifically to generate data to improve flow modeling of relaminarization on swept leading edges under high-lift conditions. This is, to our knowledge, the first time some key features of relaminarization and subsequent retransition on swept wings have been documented under controlled wind-tunnel conditions.

Virtually all flow conditions with $\bar{R} > 250$ (about eight test cases) showed strong evidence of relaminarization at the wind-tunnel chord Reynolds number of 1.3×10^6. Relaminarization is accompanied by a certain reduction in shear-stress fluctuation levels depending on the acceleration history and maximum values of K_s attained. The results on wing A have shown a spectacular decrease in the intermittency to values less than 0.2, which is caused by the large acceleration leading to maximum values of K_s of about 9×10^{-6}. On wing B, the decrease in γ levels was relatively less ($\gamma \sim 0.70$), consistent with lower maximum values of K_s. In all the relaminarized flows, retransition of the (relaminarized) boundary layer was triggered by the presence of a laminar-separation bubble, which occurred just downstream of the peak suction location on the wing. The present data set (at a chord Reynolds number of 1.3×10^6) suggests that relaminarization at a swept leading edge can occur for maximum values of K_s greater than about 3×10^{-6}. Flight Reynolds numbers are often associated with appreciably larger maximum values of K_s (8–10 $\times 10^{-6}$) and therefore may often be expected to result in relaminarization.

The present results and those obtained in flight on a Boeing 737-100 aircraft indicate that K_s is a useful parameter for correlating the occurrence of RL on swept leading edges; but K_s would have to be in excess of about 6×10^{-6} to result in relatively low intermittency in the relaminarized boundary layer. For these flows, separation bubbles following the relaminarization are well correlated with separation bubbles in more pristine laminar boundary layers; the bubble length can be estimated based on the transition Reynolds number.

Based on the present work, the following guidelines emerge from the point of view of flow modeling: For given wing and flow conditions, if the value of K_s exceeds, say 3×10^{-6}, then RL of the mean flow with moderate values of intermittency is likely. In such cases, it is meaningful to run laminar boundary-layer calculations from the attachment line (although the ATL is turbulent) for the wing upper surface and trigger transition in the calculation across the LSB or at the beginning of the adverse pressure gradient following the suction peak. The preceding suggestion presumes that retransition is not caused by crossflow instabilities, which should of course be verified.

Acknowledgements

This research was funded by the Boeing Commercial Airplane Group, Seattle, WA. R. Narasimha acknowledges support from the Defence Research and Development Organisation (DRDO), India, through a project on flow instabilities.

References

[1] Meredith, P. T., *Viscous Phenomena Affecting High-Lift Systems and Suggestions for Future CFD Development*, CP-515, AGARD, 1993, Paper 19.

[2] Yip, L. P., Vijgen, P. M. H. W., and Hardin, J. D., "In Flight Surface Flow Measurements of a Subsonic Transport High-Lift Flap System,"

International Council of the Aeronautical Sciences Paper 92-3.7.3, 1992.

[3] Van Dam, C. P., Vijgen, P. M. H. W., Yip, L. P., and Potter, R. C., "Leading-Edge Transition and Relaminarization Phenomena on a Subsonic High-Lift System," AIAA Paper 93-3140, 1993.

[4] Pfenninger, W., "Flow Phenomena at the Leading Edge of Swept Wings," Recent Development in Boundary Layer Research, AGARDograph 97, Belgium, 1965.

[5] Cumpsty, N. A., and Head, M. R., "The Calculation of Three-Dimensional Turbulent Boundary Layers, Part 2: Attachment-Line Flow on an Infinite Swept Wing," *Aeronautical Quarterly*, Vol. 18, No. 2, 1967, pp. 150–164.

[6] Poll, D. I. A., "Transition in the Infinite Swept Attachment-Line Boundary Layer," *Aeronautical Quarterly*, Vol. 30, No. 4, 1979, pp. 607–629.

[7] Arnal, D., and Juillen, J. C., "Leading-Edge Contamination and Relaminarization on a Swept Wing at Incidence," *Proceedings of Numerical and Physical Aspects of Aerodynamic Flows IV*, edited by T. Cebeci, Springer–Verlag, Berlin, 1990, pp. 391–415.

[8] Beasly, J. A., "Calculation of the Laminar Boundary Layer and Prediction of Transition on a Sheared Wing," Royal Aircraft Establishment Rept. 3787, Farnborough, U.K., 1976.

[9] Hardy, D. C., *Experimental Investigation of Attachment-Line Transition in Low Speed High-Lift Wind Tunnel Testing*, CP-438, AGARD, 1989, Paper 2.

[10] Van Dam, C. P., Los, S. M., Miley, S. J., Roback, V. E., Yip, L. P., Bertelrud, A., and Vijgen, P. M. H. W., "In-Flight Boundary Layer State Measurements on a High-Lift System," *Journal of Aircraft*, Vol. 34, No. 6, 1997, pp. 748–756.

[11] Van Dam, C. P., Los, S. M., Miley, S. J., Roback, V. E., Yip, L. P., Bertelrud, A., and Vijgen, P. M. H. W., "In-Flight Boundary Layer State Measurements on a High-Lift System: Main Element and Flap," *Journal of Aircraft*, Vol. 34, No. 6, 1997, pp. 757–763.

[12] Hansen, H., Thiede, P., Moens, F., Rudnik, R., and Quest, J., "Overview about European High-Lift Research Programme EUROLIFT," AIAA Paper 2004-767, 2004.

[13] Seraudie, A., Perraud, J., and Moens, F., "Transition Measurement and Analysis on a Swept Wing in High-Lift Configuration," *Aerospace Science and Technology*, Vol. 7, No. 8, 2003, pp. 569–576.

[14] Perraud, J., Seraudie, A., and Moens, F., "Transition on a High-Lift Swept Wing in the European Project EUROLIFT," *Journal of Aircraft*, Vol. 41, No. 5, 2004, pp. 1183–1190.

[15] Mukund, R., Viswanath, P. R., and Crouch, J. D., "Relaminarization and Retransition of Accelerated Turbulent Boundary Layers on a Convex Surface," *Proceedings of International Union of Theoretical and Applied Mechanics Symposium on Laminar-Turbulent Transition*, edited by H. F. Fasel and W. S. Saric, Springer, Sedona, AZ, 1999, pp. 243–248.

[16] Mukund, R., "Relaminarization in a Short Acceleration Zone On a Convex Surface," Ph.D. Thesis, Dept. of Aerospace Engineering, Indian Institute of Science, Bangalore, India, 2002.

[17] Mukund, R., Viswanath, P. R., Narasimha, R., and Crouch, J. D., "Relaminarization in Highly Favorable Pressure Gradients on a Convex Surface," *Journal of Fluid Mechanics* (to be published).

[18] Van Den Berg, B., "Boundary Layer Measurements on a Two-Dimensional Wing with Flap," National Aerospace Lab., TR 79009 U, Amsterdam, The Netherlands, 1979.

[19] Jahanmeri, M., Rudra Kumar, S., and Prabhu, A., "A Method for Generating Turbulent Intermittency Function," Indian Institute of Science, Rept. 91 FM13, Dept. Aerospace Engineering, Bangalore, India, 1991.

[20] Narasimha, R., and Sreenivasan, K. R., "Relaminarization of Fluid Flows," *Advances in Applied Mechanics*, Vol. 19, 1979, p. 221.

[21] Narasimha, R., and Sreenivasan, K. R., "Relaminarization in Highly Accelerated Turbulent Boundary Layers," *Journal of Fluid Mechanics*, Vol. 61, No. 3, 1973, pp. 417–447.

[22] Crouch, J. D., and Saric, W. S., "Oscillating Hot-Wire Measurements above an FX63-137 Airfoil," AIAA Paper 86-0012, 1986.

[23] Davis, R. L., Carter, J. E., and Reshotko, E., "Analysis of Transitional Separation Bubbles on Infinite Swept Wings," AIAA Paper 85-1685, 1985.

[24] Roberts, W. B., "A Study of the Effect of Reynolds Number and Laminar Separation Bubbles on the Flow Through Axial Compressor Cascades," D.Sc. Thesis, Univ. Libre de Bruxelles and VKI, Brussels, May 1973.

[25] Roberts, W. B., "Calculation of Laminar Separation Bubbles and Their Effect on Airfoil Performance," *AIAA Journal*, Vol. 18, No. 1, 1980, pp. 25–30.

N. Chokani
Associate Editor